

## DOCKING STUDY OF MOLECULAR MECHANISM BEHIND THE QUERCETIN INHIBITION OF *MYCOBACTERIUM TUBERCULOSIS* UREASE

Lisnyak Yu. V., Martynov A. V.

Mechnikov Institute of Microbiology and Immunology

### Introduction

*Mycobacterium tuberculosis* urease (MTU) belongs to a group of nickel-dependent metalloenzymes (urea amidohydrolase, EC 3.5.1.5) [1-4]. MTU, being an important factor of the bacterium viability and virulence [5, 6], is an attractive target for anti-tuberculosis drugs acting by inhibition of urease activity. However, known urease inhibitors (phosphorodiamidates, hydroxamic acid derivatives and imidazoles) are toxic and/or unstable, that prevent their clinical use [7-9]. Therefore, the development of novel efficient and safe MTU inhibitors is necessary. To achieve this goal, we have chosen flavonoid quercetin (fig. 1) as a scaffold to develop new MTU inhibitors.

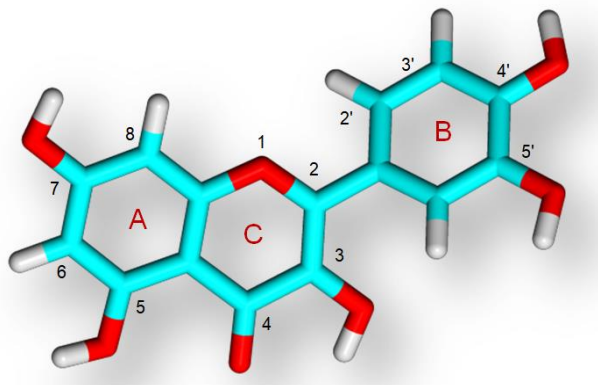


Fig. 1. Quercetin.

Owing to the presence of multiple polar groups and certain conformational flexibility it may form multiple hydrogen bonds while adapting to the binding site environment. Also, quercetin was shown to be a noncompetitive inhibitor of *Helicobacter pylori* urease [10] and a strong time-dependent inhibitor of *Klebsiella aerogenes* urease [11].

This paper aimed to docking study the molecular mechanism behind the quercetin inhibition of *Mycobacterium tuberculosis* urease.

### Methods

**Homology modeling.** Homology model of *M. tuberculosis* urease was built as described earlier [12] by

using molecular modeling program YASARA Structure [13]. The target amino acid sequence of *M. tuberculosis* H37Rv urease was taken from GenBank at NCBI [14]. Amongst the top-scoring templates, five high-resolution X-ray structures for the following bacterial ureases were selected: *K. aerogenes* (2KAU), *S. pasteurii* (5G4H, 4UBP and, 4CEU), and *E. aerogenes* (4EPB). For each template five stochastic alignments were created and for each alignment a three-dimensional model was built. Each model was energy minimized with explicit water molecules using Yasara2 force field [13], and the models were ranked by quality Z-score. From these 25 three-dimensional models obtained, there was selected a model based on the template X-ray high-resolution structure for *S. pasteurii* urease (5G4H) which contained the flap in open state and had the highest quality score amongst the nonamer structures (i.e.  $(\alpha\beta\gamma)_3$  macromolecular ensembles).

**Search of inhibitor binding sites on the surface of MTU.** The search of inhibitor binding sites on the surface of MTU was carried out by two steps. At first step, we used computational solvent mapping method FTSite [15] to identify a ligand binding sites on MTU surface. At second step, docking of quercetin on MTU surface by AutoDock Vina [16] implemented in YASARA Structure was carried out within the ligand binding sites revealed by FTSite. Such strategy allowed to speed up the docking and increase the search accuracy by limiting the search space.

**Mapping of protein surface by FTSite method.** Computational solvent mapping method FTSite was used through the online server [17]. The method is based on the concept of "hot spots", i.e. the regions of protein binding sites that major contribute to the binding free energy and, hence, are prime targets in drug design [18-20]. The FTSite method places molecular probes, small organic molecules containing various functional groups, on a dense grid defined around the protein, and for each probe finds favorable positions by rigid body search using empirical free energy functions. The selected poses are refined by free energy minimization, the low energy conformations are clustered, and the clusters are ranked on the basis of the average free energy [15, 17, 20]. To determine the hot spots, there are found the so called consensus sites, i.e. regions on the protein that bind several different probe clusters, and these sites are ranked by the number of nonbound contacts between the protein and all probes in the consensus cluster. The consensus cluster with the highest number of contacts is ranked first. The amino acid residues in contact with the probes of this cluster constitute the top ranked predicted ligand binding site. Clusters with fewer contacts define lower ranked predictions [17]. To evaluate the clusters of bound probe molecules, there were used energy functions that account for non-bonded van der Waals and electrostatic interactions, as well as solvation effects [15, 17, 20]. FTSite server outputs the protein residues delineating the first three binding sites.

**Molecular docking by AutoDock VINA.** Docking of quercetin on the surface of *M. tuberculosis* urease by

AutoDock VINA was carried within the binding sites previously revealed by FTSite server as described above. Docking was performed by using default parameters within a cubic 30 Å × 30 Å × 30 Å simulation cell centered on S atom of Cys 532 residue. The *M. tuberculosis* urease structure was kept rigid while the ligand structure was flexible. The best hit of 25 runs having the lowest binding energy was chosen as a final binding pose.

An analysis of molecular interactions and a representation of the results by molecular graphics were done by YASARA Structure [13], LigPlot+ [21] and PyMol [22].

## Results and discussion

**Mapping of *M. tuberculosis* urease surface by FTSite method.** The results of FTSite mapping are shown in fig. 2A where binding sites are delineated by corresponding residues and colored in accord with the site rank: red, green and blue for the first, second and third binding site, respectively. Residues constituted MTU ligand-binding sites 1-3 summarized in table 1.

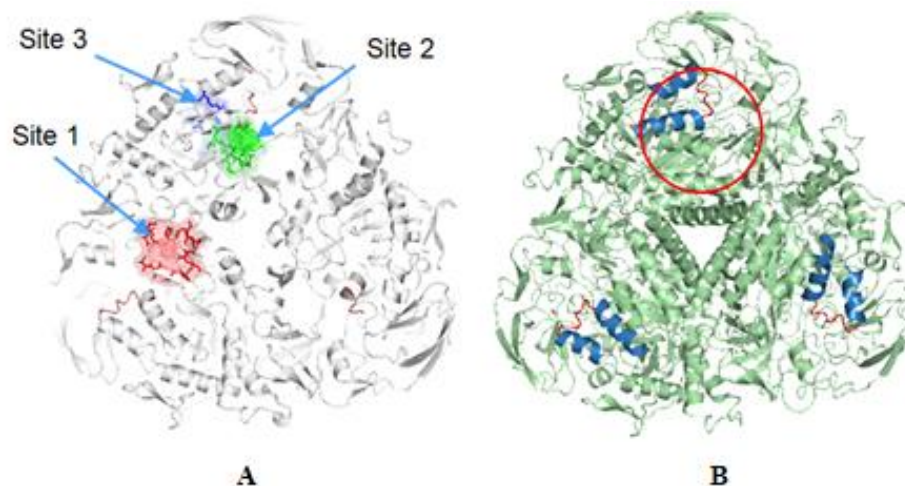


**Fig. 2. Ligand-binding sites of *M. tuberculosis* urease. A - Ligand-binding sites revealed by FTSite. B – Equivalent combined binding site (marked by red circle) comprising all three binding sites revealed by FTSite within one heterotrimer.**

**Table 1. Ligand-binding sites of MTU revealed by FTSite.**

Site 1	Site 2	Site 3
HIS A 32	ILE C 351	HIS C 349
ILE A 36	LYS C 379	THR C 380
MET A 76	THR C 380	HIS C 432
LEU A 77	VAL C 531	HIS C 459
ALA A 78	CYS C 532	HIS C 485
GLU A 79	GLN C 575	GLY C 490
VAL A 80	ALA C 576	ARG C 549
GLN A 81	MET C 577	ASP C 573
GLU C 652	GLN D 81	ALA C 576
THR C 683	ILE F 681	MET C 577
PRO C 684	PRO F 682	
GLN C 685	THR F 683	
VAL C 687		
MET D 1		
ARG D 2		

As can be seen from table 1, unlike site 3 which is the active site and contains only residues belonging to C-chain, the sites 1 and 2 are composed of residues not overlapping with ones of the active site and belonging to various chains: A, C and D (site 1) and C, D and F (site 2). These features are usually characteristic for allosteric sites.

Taking into account the symmetry of urease's homotrimers of heterotrimers, binding site 1 can be symmetrically transferred to heterotrimer containing sites 2 and 3 to get equivalent combined site comprising all three binding sites within a single heterotrimer. This combined site may be approximated by a sphere of radius 30 Å with a center near residue Cys 532 (fig. 2B).

**Docking of quercetin by AutoDock Vina.** In the best binding pose, quercetin molecule is situated deep in the

MTU cavity which leads to the active site channel and near the active site flap (fig. 3). The circle B of quercetin is directed to the active center, while the circle A is directed towards the exit from the cavity. Binding energy and dissociation constant of quercetin complex with urease is 8.7 Kcal/mol and 0.4 μM, correspondingly. Ligand efficiency equals 0.4. The binding of quercetin is provided by tight van der Waals contacts with eleven residues (fig. 4A) two of which (Cys 532 and His 533) belong to the active site flap modulating transit of substrate and products of catalysis through the active site channel. The binding of quercetin is additionally stabilized by six hydrogen bonds with residues Glu 376, Lys 379, Thr 380, Gly 490 and Ala 576 (Fig. 4B).

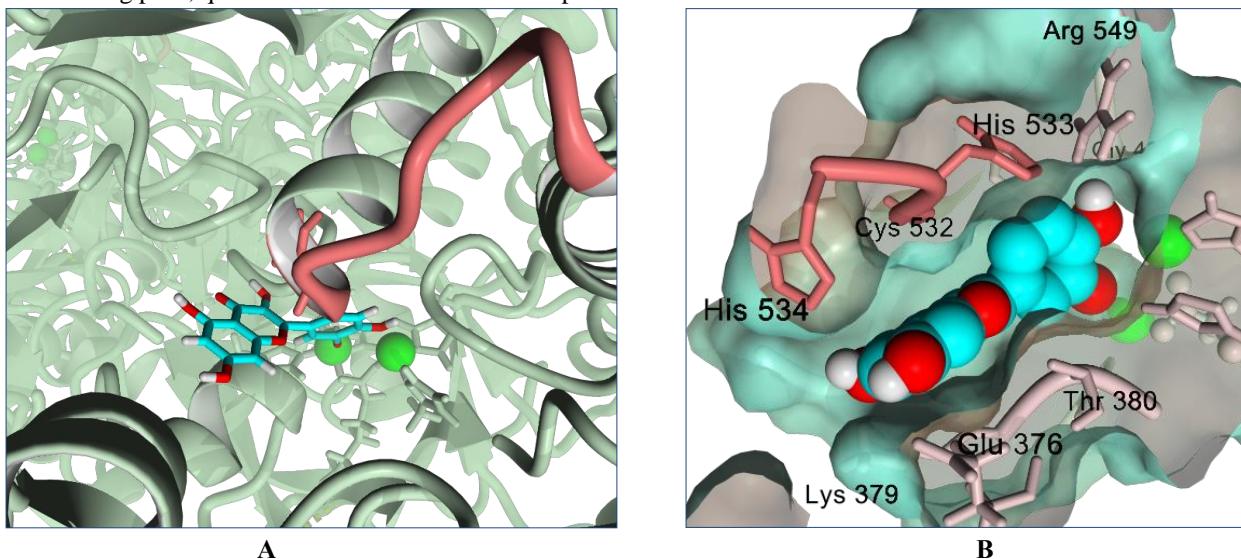


**Fig. 3.** Quercetin position relative to active center and flexible flap of MTU: general view (A) and cross section of MTU molecular surface (B). Ni atoms are green colored, and flexible flap is colored in deep salmon.

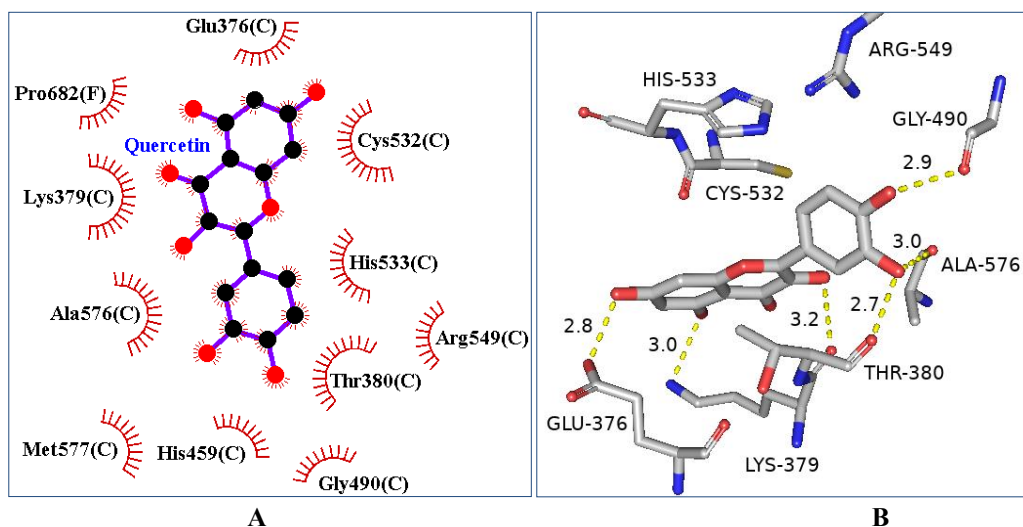


**Fig. 4.** Intermolecular interactions of quercetin with MTU: van der Waals interactions (A) and H-bonds (B).

These intermolecular interactions (through the tight contact with flap residues Cys 532 and, especially His 533) cause steric hindrance for the flap transition from open to closed conformation thus fixing it in the open state that blocks catalysis. As can be seen from the superposition of quercetin-MTU complex with the open flap and experimental structure of *Sporosarcina pasteurii* urease

(PDB code 2UBP) with the closed flap, in quercetin-MTU complex quercetin molecule is placed at the position that His 533 residue occupies if the active site flap is in the closed conformation (fig. 5).

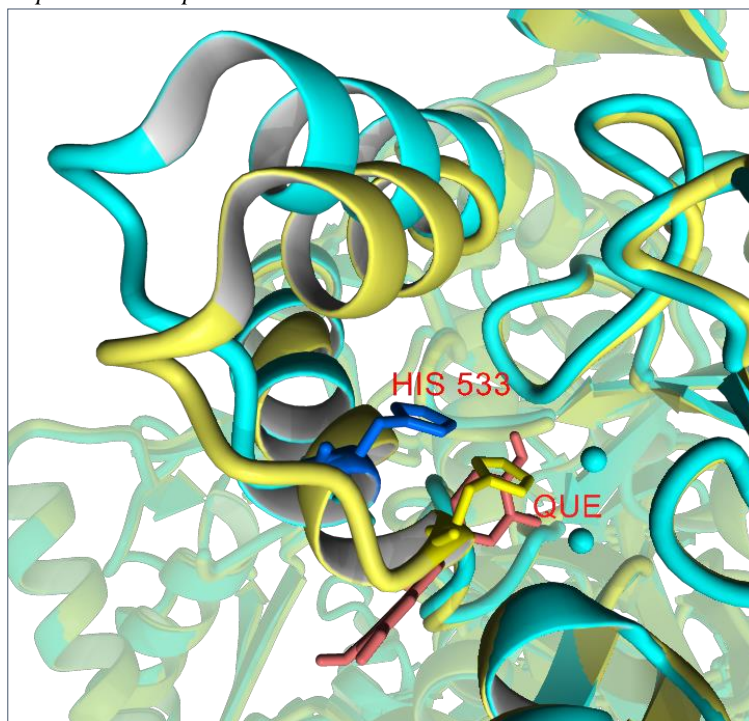


**Fig. 5.** Superposition of quercetin-MTU complex with open flap (cyan colored) and experimental structure of *Sporosarcina pasteurii* urease (PDB code 2UBP) with closed flap (yellow colored). In these structures, equivalent His residues, as well as quercetin molecule are shown as stick models colored in blue, yellow and deep salmon, respectively.

Our model of quercetin binding to MTU corresponds to the results of Xiao Z.-P. et al. which showed by enzyme kinetics and molecular docking that quercetin is a noncompetitive inhibitor of *Helicobacter pylori* urease and it is positioned near the active site flap as well blocking it in the open conformation [10]. Recently, Macomber L. et al. showed by docking that quercetin binds to the flap region of *Klebsiella aerogenes* urease too, and they suggested that quercetin further form a covalent attachment to Cys 319 (Cys 319 corresponds to Cys 532 residue of *M. tuberculosis* urease) [11]. This assumption was soon partially confirmed by Mazzei L. et al. [23]. They obtained the high resolution X-ray structure of *Sporosarcina pasteurii* urease inactivated by catechol (benzene-1,2-diol), the simplest polyphenol compound that may be considered as a part of quercetin molecular structure (see circle B in fig.1). In this complex,

catechol is covalently bound to Cys 322 located on the active site flap and block it in the open position (Cys 322 corresponds to Cys 532 residue of *M. tuberculosis* urease). The authors supposed that it is a general feature common to aromatic poly-hydroxylated urease inhibitors [23].

It should be noted that in our complex of quercetin with *M.tuberculosis* urease the quercetin molecule, especially its C-ring, is close to the position of both Cys 532 residue (fig. 3 B) and catechol in experimental structure of *S. pasteurii* urease complex with catechol (fig. 6). Thus, our model of quercetin binding to *M. tuberculosis* urease does not exclude the possibility for quercetin, being near Cys 532 residue, to form a covalent bond with it.

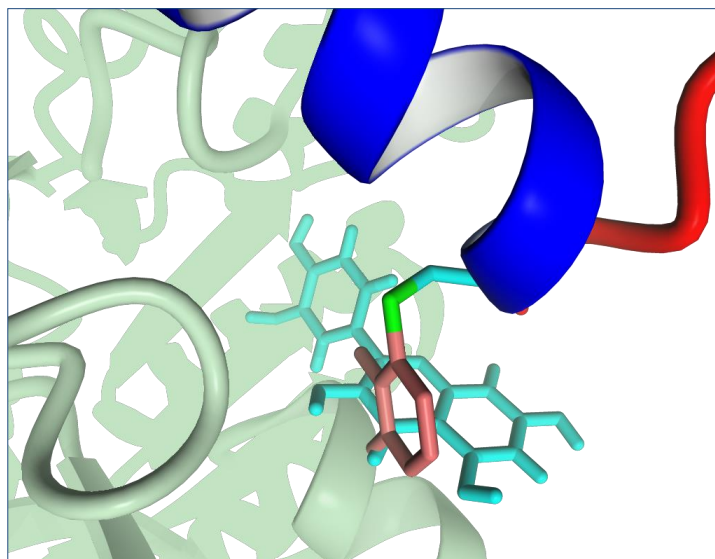


**Fig. 6. Superposition of quercetin binding pose (cyan colored) on catechol-*S.pasteurii* urease complex. Catechol colored in deep salmon is bound to flap's Cys residue. Helix motif and mobile part of the flap of *S. pasteurii* urease are blue and red colored, respectively.**

## Conclusions

Because of the absence of experimental structure of *M. tuberculosis* urease its homology model was built and used in further studies of ligand-urease interactions. It was revealed that quercetin molecule is situated in the MTU cavity leading to the active site channel, near the active site flap. The binding of quercetin is provided by van der Waals contacts with eleven residues and by six hydrogen bonds with urease residues. Based on the analysis of peculiarities of quercetin binding to MTU, molecular mechanism of MTU inhibition by quercetin was proposed. The model of quercetin binding to MTU corresponds well to the results of docking studies on quercetin binding to *Helicobacter pylori* and *Klebsiella aerogenes* ureases. The results obtained expand the knowledge on the molecular mechanisms of urease inhibition and contribute to the development of new anti-tuberculosis immunomodulators.

## References

1. Dixon, N. E. 1975. Jack bean urease (EC 3.5.1.5). A metalloenzyme. A simple biological role for nickel? / N. E. Dixon, C. Gazzola, R. L. Blakeley, B. Zerner. // J. Am. Chem. Soc. 1975. Vol. 97. P. 4131-4133.
2. Ragsdale, S. W. Nickel-based enzyme systems / S.W. Ragsdale // J. Biol. Chem. 2009. Vol. 284, N 28. P. 18571-18575.
3. Carter, E. L. Interplay of metal ions and urease / E. L. Carter, N. Flugga, J. L. Boer, S. B. Mulrooney, R. P. Hausinger // Metallomics. 2009. Vol. 1. P. 207-221.
4. Boer, J. L. Nickel-dependent metalloenzymes / J. L. Boer, S. B. Mulrooney, R. P. Hausinger // Arch. Biochem. Biophys. 2014. Vol. 544. P. 142-152.
5. Mobley, H. L. T. Molecular biology of microbial ureases / H. T. Mobley, M. D. Island, R. P. Hausinger // Microbiol. Rev. 1995. Vol. 59. N 3. P. 451-480.
6. Mobley, H. L. T. Microbial ureases: significance, regulation, and molecular characterization / H. L. T. Mobley, R. P. Hausinger // Microbiol. Rev. 1989. Vol. 53. N 1. P. 85-108.
7. Modolo, L. V. An overview on the potential of natural products as urease inhibitors: a review / L. V. Modolo, A. X. de Souza, L. P. Horta, D. P. Araujo, A. de Fatima // J. Adv. Res. 2015. Vol. 6. P. 35-44.
8. Azizian, H. Large-scale virtual screening for the identification of new *Helicobacter pylori* urease inhibitor scaffolds / H. Azizian, F. Nabati, A. Sharifi, F. Siavoshi, M. Mahdayi, M. Amanlou // J. Mol. Model. 2012. Vol. 18. P. 2917-2927.
9. Ibrar A, Khan I, Abbas N. Structurally diversified heterocycles and related privileged scaffolds as potential urease inhibitors: a brief overview / A. Ibrar, I. Khan, N. Abbas // Arch. Pharm. Chem. Life Sci. 2013. Vol. 346. P. 423-446.
10. Xiao, Z.-P. Molecular docking, kinetic study and structure-activity relationship analysis of quercetin and its analogues as *Helicobacter pylori* urease inhibitors / Z.-P. Xiao, X.-J. Wang, Z.-Y. Peng, S. Huang et al. // J. Agric. Food Chem. 2012. Vol. 60. P. 10572-10577.
11. Macomber, L. Reduction of urease activity by interaction with the flap covering the active site / L. Macomber, M. S. Minkara, R. P. Hausinger, K. M. Merz, Jr. // J. Chem. Inf. Model. 2015. Vol. 55. P. 354-361.
12. Lisnyak, Yu. V. Homology modeling and molecular dynamics study of *Mycobacterium tuberculosis* urease / Yu. V. Lisnyak, A. V. Martynov // Annals of Mechnikov's Institute. 2017. № 3. P. 23-36.

13. Kreiger, E. Improving physical realism, stereochemistry, and side-chain accuracy in homology modelling: four approaches that performed well in CASP8 / E. Kreiger, K. Joo, J. Lee, et al. // *Proteins*. 2009. Vol. 77, Suppl. 9. P. 114-122.
14. Benson, D. A. GenBank / D. A. Benson, I. Karsch-Mizrachi, D. J. Lipman, J. Ostell, D. L. Wheeler // *Nucl. Acids Res.* 2007. Vol. 35, Suppl 1. P. D21- D25.
15. Ngan, C.-H. FTSite: high accuracy detection of ligand binding sites on unbound protein structures / C. H. Ngan, D. R. Hall, B. Zerbe, L. E. Grove, D. Kozakov, S. Vajda // *Bioinformatics*. 2012. Vol. 28, N 2. P. 286- 287.
16. Trott, O. AutoDock Vina: improving the speed and accuracy of docking with a new scoring function, efficient optimization and multithreading / *J. Comput. Chem.* 2010. Vol. 31, N 2. P. 455-461.
17. Kozakov, D. The FT. Map family of web servers for determining and characterizing ligand-binding hot spots of proteins / D. Kozakov, L. E. Grove, D. R. Hall, T. Bohnuud et al. // *Nature Protocols*. – 2015. Vol. 10, N 15. P. 733-755.
18. Brenke, R. Fragment-based identification of druggable "hot spots" of proteins using Fourier domain correlation techniques / R. Brenke, D. Kozakov, G.-Y. Chuang, D. Beglov, D. Hall, M. R. Landon, C. Mattos, S. Vajda // *Bioinformatics*. 2009. Vol. 25. P. 621–627.
19. Landon, M. R. Identification of hot spots within druggable binding sites of proteins by computational solvent mapping / M. R. Landon, D. R. Lancia Jr, J. Yu, S. C. Thiel, S. Vajda // *J. Med. Chem.* 2007. Vol. 50. P. 1231-1240.
20. Silberstein, M. Identification of substrate binding sites in enzymes by computational solvent mapping / M. Silberstein, S. Dennis, III L Brown, T. Kortvelyesi, K. Clodfelter, S. Vajda // *J. Mol. Biol.* 2003. Vol. 332. P. 1095-1113.
21. Laskowski, R. A. LigPlot+: multiple ligand-protein interaction diagrams for drug discovery / R. A. Laskowski, M. B. Swindells // *J. Chem. Inf. Model.* 2011. Vol. 51. P. 2778-2786.
22. The PyMOL Molecular Graphics System, Version 2.0 Schrödinger, LLC.
23. Mazzei, L. Inactivation of urease by catechol: kinetics and structure / L. Mazzei, M. Cianci, F. Musiani, G. Lente, et al. // *J. Inorg. Biochem.* 2016. Vol. 166. P. 182-189.

### DOCKING STUDY OF MOLECULAR MECHANISM BEHIND THE QUERCETIN INHIBITION OF MYCOBACTERIUM TUBERCULOSIS UREASE

Lisnyak Yu. V., Martynov A. V.

**Introduction.** *Mycobacterium tuberculosis* urease (MTU), being an important factor of the bacterium viability and virulence, is an attractive target for anti-tuberculosis drugs acting by inhibition of urease activity. However, known urease inhibitors (phosphorodiamidates, hydroxamic acid derivatives and imidazoles) are toxic and/or unstable, that prevent their clinical use. Therefore, the development of novel efficient and safe MTU inhibitors is necessary. To achieve this goal, we have chosen

flavonoid quercetin as a scaffold to develop new MTU inhibitors. **Methods. Homology modeling.** The target amino acid sequence of *M. tuberculosis* H37Rv urease was taken from GenBank at NCBI. Homology model of *M. tuberculosis* urease was built as described earlier by using molecular modeling program YASARA Structure. Amongst the top-scoring templates, five high-resolution X-ray structures were selected. For each template five stochastic alignments were created and for each alignment a three-dimensional model was built. Each model was energy minimized with explicit water molecules using Yasara2 force field, and the models were ranked by quality Z-score. From these 25 three-dimensional models obtained, there was selected a model based on the template X-ray high-resolution structure for *S. pasteurii* urease (5G4H) which contained the flap in open state and had the highest quality score amongst the nonamer structures (i.e.  $(\alpha\beta\gamma)_3$  macromolecular ensembles). **Search of inhibitor binding sites on the surface of MTU.** The search of inhibitor binding sites on the surface of MTU was carried out by two steps. At first step, we used computational solvent mapping method FTSite to identify a ligand binding sites on MTU surface. At second step, docking of quercetin on MTU surface by AutoDock Vina implemented in YASARA Structure was carried out within the ligand binding sites revealed by FTSite. **Mapping of protein surface by FTSite method.** Computational solvent mapping method FTSite was used through the online server. FTSite server outputs the protein residues delineating the first three binding sites. **Molecular docking by AutoDock VINA.** Docking of quercetin on the surface of *M. tuberculosis* urease by AutoDock VINA was carried within the binding sites previously revealed by FTSite server. Docking was performed by using default parameters within a cubic  $30 \text{ \AA} \times 30 \text{ \AA} \times 30 \text{ \AA}$  simulation cell centered on S atom of Cys 532 residue. The *M. tuberculosis* urease structure was kept rigid while the ligand structure was flexible. The best hit of 25 runs having the lowest binding energy was chosen as a final binding pose. An analysis of molecular interactions and a representation of the results by molecular graphics were done by YASARA Structure, LigPlot+ and PyMol. **Results and discussion.** In the best binding pose, quercetin molecule is situated deep in the MTU cavity which leads to the active site channel and near the active site flap. The circle B of quercetin is directed to the active center, while the circle A is directed towards the exit from the cavity. Binding energy and dissociation constant of quercetin complex with urease is 8.7 Kcal/mol and 0.4  $\mu\text{M}$ , correspondingly. Ligand efficiency equals 0.4. The binding of quercetin is provided by tight van der Waals contacts with eleven residues two of which (Cys 532 and His 533) belong to the active site flap modulating transit of substrate and products of catalysis through the active site channel. The binding of quercetin is additionally stabilized by six hydrogen bonds with residues Glu 376, Lys 379, Thr 380, Gly 490 and Ala 576. These intermolecular interactions (through the tight contact with flap residues Cys 532 and,

especially His 533) cause steric hindrance for the flap transition from open to closed conformation thus fixing it in the open state that blocks catalysis. Our model of quercetin binding to MTU corresponds to the results of Xiao Z.-P. et al. which showed by enzyme kinetics and molecular docking that quercetin is a noncompetitive inhibitor of *Helicobacter pylori* urease and it is positioned near the active site flap as well blocking it in the open conformation. As well, our model of quercetin binding to urease corresponds to the results of Macomber L. et al. which showed by docking that quercetin binds to the flap region of *Klebsiella aerogenes* urease. However, our model disagrees with the proposed general mechanism of urease inhibition by aromatic poly-hydroxylated inhibitors through the covalent binding with Cys residue of the flap covering the active site. It may be a consequence of the limitation of molecular docking methods used in our study that can explore only non-bound interactions. **Conclusions.** Because of the absence of experimental structure of *M. tuberculosis* urease its homology model was built and used in further studies of ligand-urease interactions. It was revealed that quercetin molecule is situated in the MTU cavity leading to the active site channel, near the active site flap. The binding of quercetin is provided by van der Waals contacts with eleven residues and by six hydrogen bonds with urease residues. Based on the analysis of peculiarities of quercetin binding with MTU, molecular mechanism of MTU inhibition by quercetin was proposed. The model of quercetin binding with MTU corresponds well to the results of docking studies on quercetin binding to *Helicobacter pylori* and *Klebsiella aerogenes* ureases. The results obtained expand the knowledge on the molecular mechanisms of urease inhibition and contribute to the development of new anti-tuberculosis immunomodulators.

**Key words:** *Mycobacterium tuberculosis* urease, urease inhibitors, quercetin, molecular docking.